Table 8 *Continued*

Indicator/use	*Function*	
	Pros	*Cons*
Caffeine	May be specific to sewage, but unproven to date Could be developed into a dipstick assay	Yet to be proven as a reliable method
Detergents (calcufluors)	Relatively routine methods available	May not be related to sewage (e.g., industrial pollution)
Turbidity	Simple, direct, and inexpensive assay available in the field	May not be related to sewage; correlation must be shown for each site type
Cryptosporidium (animal source pathogens)	Required for potential zoonoses, such as *Cryptosporidium* spp., where fecal indicator bacteria may have died out, or are not present	Expensive and specialized assay (e.g., Method 1622, USEPA) Human/animal speciation of serotypes not currently defined

Reproduced with permission from Bartram and Rees (2000).

Table 9 Primary classification matrix

Sanitary inspection category (susceptibility to fecal influence)	*Microbiological assessment category* (indicator counts)				
	A	*B*	*C*	*D*	*E*
Very low	Excellent	Excellent	Good	Good (+)	Fair (+)
Low	Excellent	Good	Good	Fair	Fair (+)
Moderate	Good[a]	Good	Fair	Fair	Poor
High	Good[a]	Fair[a]	Fair	Poor	Very poor
Very high	Fair[a]	Fair[a]	Poor[a]	Very poor	Very poor

[a] Unexpected result requiring verification.
(+) implies non-sewage sources of fecal indicators (e.g., livestock) and this should be verified.
Reproduced with permission from Bartram and Rees (2000).

See also

Pollution Control. Sandy Beaches, Biology of.

Further Reading

Bartram J and Rees G (eds) (2000) *Monitoring Bathing Waters*. London: E&FN Spon.

Bradford-Hill A (1965) The environment and disease: association or causation? *Proceedings of the Royal Society of Medicine* 58: 295–300.

Esrey S, Feachem R and Hughes J (1985) Interventions for the control of diarrhoeal diseases among young children: improving water supplies and excreta disposal facilities. *Bulletin of the World Health Organization* 63(4): 757–772.

Ludwig RG (1988) *Environmental Impact Assessment. Siting and Design of Submarine Outfalls*. An EIA Guidance Document. MARC Report No. 43. Geneva: Monitoring and Assessment Research Centre/World Health Organization.

Mara D and Cairncross S (1989) *Guidelines for the Safe Use of Wastewater and Excreta in Agriculture and Aquaculture*. Geneva: WHO.

WHO (1998) *Guidelines for Safe Recreational-water Environments: Coastal and Freshwaters*. Draft for Consultation. Document EOS/DRAFT/98.14 Geneva: World Health Organization.

VOLCANIC HELIUM

J. E. Lupton, Hatfield Marine Science Center, Newport, OR, USA

doi:10.1006/rwos.2001.0165

Introduction

Volcanic activity along the global mid-ocean ridge system and at active seamounts introduces a helium-rich signal into the ocean basins that can be used to trace patterns of ocean circulation and mixing. Helium is extracted from oceanic volcanic rocks by circulating sea water and then injected into the ocean as helium dissolved in submarine hydrothermal vent fluids. Hydrothermal venting produces plumes in the ocean that are highly enriched in a variety of tracers, including heat, helium, manganese, iron, methane, and hydrogen. Among these, volcanic helium is a particularly useful tracer because it has such a high concentration in hydrothermal fluids relative to the background values of helium in sea water, and because it is stable and conservative, i.e., helium does not decay radioactively and is not affected by any chemical or biological processes. By making careful measurements of the relative abundance of helium isotopes, it is possible to trace hydrothermal helium plumes for thousands of kilometers from the source regions.

There are two stable isotopes of helium, ^{3}He and ^{4}He, which vary in their ratio by over three orders of magnitude in terrestrial samples. The Earth's atmosphere is well mixed with respect to helium and contains helium with a uniform isotopic composition of $^3\text{He}/^4\text{He} = 1.39 \times 10^{-6}$. Atmospheric helium is a convenient standard for helium isotope determinations, and terrestrial ^{3}He/^{4}He ratios are usually normalized to the air ratio and expressed in units of R/R_A, where $R = {}^3\text{He}/^4\text{He}$ and $R_A = ({}^3\text{He}/^4\text{He})_{\text{air}}$. In contrast to atmospheric helium ($R/R_A = 1$), the radiogenic helium produced by α-decay of U and Th series isotopes has a much lower ratio of R/R_A 0.1, while the volcanic helium that is derived from the Earth's mantle is highly enriched in ^{3}He ($R/R_A = 5$–30). Thus volcanic helium has an isotopic composition distinct from other sources such as atmospheric helium or the helium produced by radioactive decay. This ^{3}He-rich mantle helium is sometimes called 'primordial' helium, since it is thought to be the remnant of a primitive component trapped in the Earth's interior since the time of its formation. This trapped component probably had $^3\text{He}/^4\text{He} = 1 \times 10^{-4}$ or 100 R_A, similar to the helium found trapped in meteorites or in the solar wind, but has been modified to $R = 30\,R_A$ by dilution with radiogenic helium since the time the Earth was formed. Although there is a wide variety of volcanic sources in the oceans, including subduction zone volcanoes and hot spot volcanoes, most of the oceanic volcanic helium is derived from activity along the global mid-ocean ridge system. While the ^{3}He/^{4}He ratio of mantle helium shows a wide range of variation, the helium from mid-ocean ridges falls in a much narrower range of $R/R_A = 7$–9.

In order of decreasing importance, the most abundant forms of helium in sea water are dissolved atmospheric helium, volcanic helium, and to a lesser degree radiogenic helium from sediments. There is also an input of pure ^{3}He into the oceans from tritium (^{3}H), the radioactive isotope of hydrogen, which decays to ^{3}He with a half-life of 12.4 years. Because tritium is generally found only in the upper ocean, ^{3}He from tritium decay (tritiogenic helium) is only significant at depths less than about 1000 m.

Although there are only two isotopes of helium, it is still possible to clearly distinguish submarine volcanic helium from the other components because of its high ^{3}He/^{4}He ratio and because volcanic helium is introduced at mid-depth rather than at the ocean surface or on the abyssal plain.

Units

For samples highly enriched in helium such as volcanic rocks and hydrothermal vent fluids, the helium isotope ratio is usually expressed in the R/R_A notation described above. However, for the relatively small variations observed in sea water samples, the ^{3}He/^{4}He variations are usually expressed as $\delta(^3\text{He})$, which is the percentage deviation from the ratio in air, defined as in eqn [1].

$$\delta(^3\text{He}) = 100[(R/R_A) - 1], \qquad [1]$$

Here again $R = {}^3\text{He}/^4\text{He}$ and $R_A = ({}^3\text{He}/^4\text{He})_{\text{air}}$. Thus $R/R_A = 1.50$ is equivalent to $\delta(^3\text{He}) = 50\%$.

History and Background

The first attempt to detect nonatmospheric helium in the oceans was made by Suess and Wänke in 1965, who predicted that the deep oceans should contain excess ^{4}He due to U and Th decay in sediments and in the ocean crust. Although they were correct about the existence of radiogenic helium in the oceans, their measurements were of insufficient precision to detect any ^{4}He enrichment above the dissolved air component. It is now known that the input of ^{3}He-rich volcanic helium has a greater effect on both the ^{3}He/^{4}He ratio and the ^{4}He concentration in sea water than does the input of radiogenic helium.

Mantle or volcanic helium was first detected on the Earth as an excess in the ^{3}He/^{4}He ratio in deep Pacific waters. Although this oceanic ^{3}He excess is derived from the helium residing in oceanic volcanic rocks, it was not until about five years later that mantle helium was directly measured in the volcanic rocks themselves. Clarke *et al.* in 1969 reported a

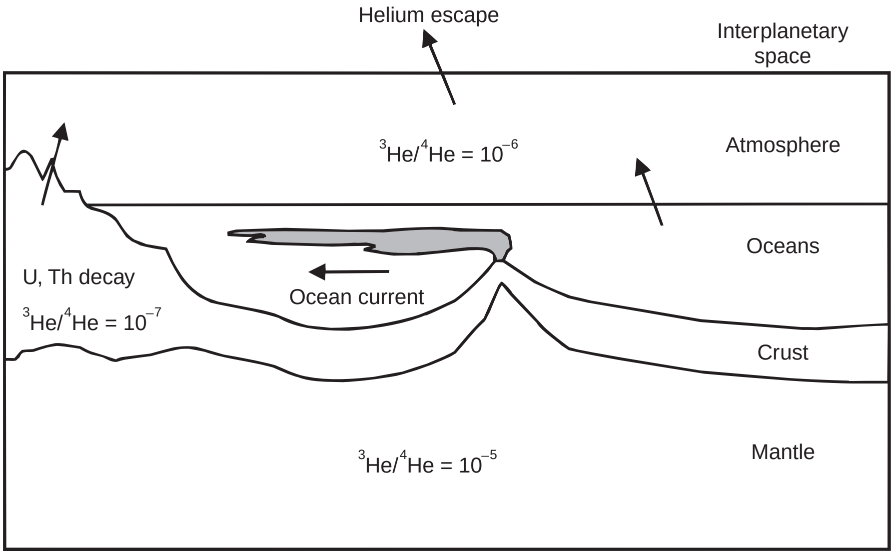

Figure 1 A schematic of the terrestrial helium budget, indicating the flux of helium from the Earth's mantle into the oceans, and in turn into the atmosphere.

21% excess in the ^{3}He concentration at mid-depth above that expected for air-saturated water, and correctly attributed this excess to a flux of primordial helium leaking from the Earth's interior into the oceans and in turn into the atmosphere (see **Figure 1**). Using a box model for oceanic helium, they were able to estimate the global ^{3}He flux from the oceans into the atmosphere at 2 atoms ^{3}He cm^{-2}, a number that is still in reasonable agreement with more recent flux estimates of 4–5 atoms ^{3}He cm^{-2}.

The discovery of excess ^{3}He in the oceans from localized sources distributed along the global mid-ocean ridge system led immediately to the use of this tracer for oceanographic studies. The Geochemical Ocean Sections Study (GEOSECS), which began in 1972, provided the first maps of the global distribution of helium in the oceans. Since then, several other oceanographic programs, including the World Ocean Circulation Experiment (WOCE), have added to our knowledge of the global helium distribution.

To illustrate the presence of volcanic helium in the oceans, a typical helium profile in the north Pacific Ocean is shown in **Figure 2**. The figure shows the vertical variation in the ^{3}He/^{4}He ratio expressed as $\delta(^3\text{He})$ in%, and the ^{4}He concentration in nmol kg^{-1}. The values expected for air-saturated water (dashed lines) are shown for comparison. For the calculation of air-saturated values it is assumed that each water parcel equilibrated with the atmosphere at the potential temperature of the sample. This profile exhibits a broad maximum in the deep water, reaching a value of $\delta(^3\text{He}) = 25.0\%$ at ~1850 m depth. Although this station is located at a distance of over 1500 km from the nearest active spreading center, the profile still exhibits a clear excess in ^{3}He/^{4}He in the 1500–3500 m depth range due to input of volcanic helium from the mid-ocean ridge system. The secondary maximum in the $\delta(^3\text{He})$ profile at ~350 m depth is due to excess ^{3}He produced by tritium decay. That this peak is tritiogenic helium is evident because the peak in $\delta(^3\text{He})$ at 350 m depth is absent from the ^{4}He profile, indicating input of pure ^{3}He as would be expected for tritium decay. At the ocean surface $\delta(^3\text{He}) = -1.4\%$, which is very close to the expected value of $\delta(^3\text{He}) = -1.35\%$ for water in equilibrium with air (^{3}He is slightly less soluble in water than ^{4}He).

The absolute ^{4}He concentration (**Figure 2B**) also increases with depth, but not as dramatically as the ^{3}He/^{4}He ratio. Part of the ^{4}He increase is due to the higher solubility of helium in the colder deep waters, as shown by the expected solubility values for air-saturated water (dashed line). However, much of the ^{4}He excess above solubility equilibrium is due to the finite amount of ^{4}He present in the volcanic helium signal. At ~2500 m depth, the profile has ^{4}He = 1.92 nmol kg^{-1}, about 10% higher than the value of 1.75 nmol kg^{-1} for air-saturated water at those conditions.

The distinct isotopic signature of oceanic volcanic helium can be seen by plotting the ^{3}He concentration versus the ^{4}He concentration as shown in **Figure 3**. In this plot the slope of the trends corresponds to the isotopic ratio of the end-member helium that has been added to the water samples. The

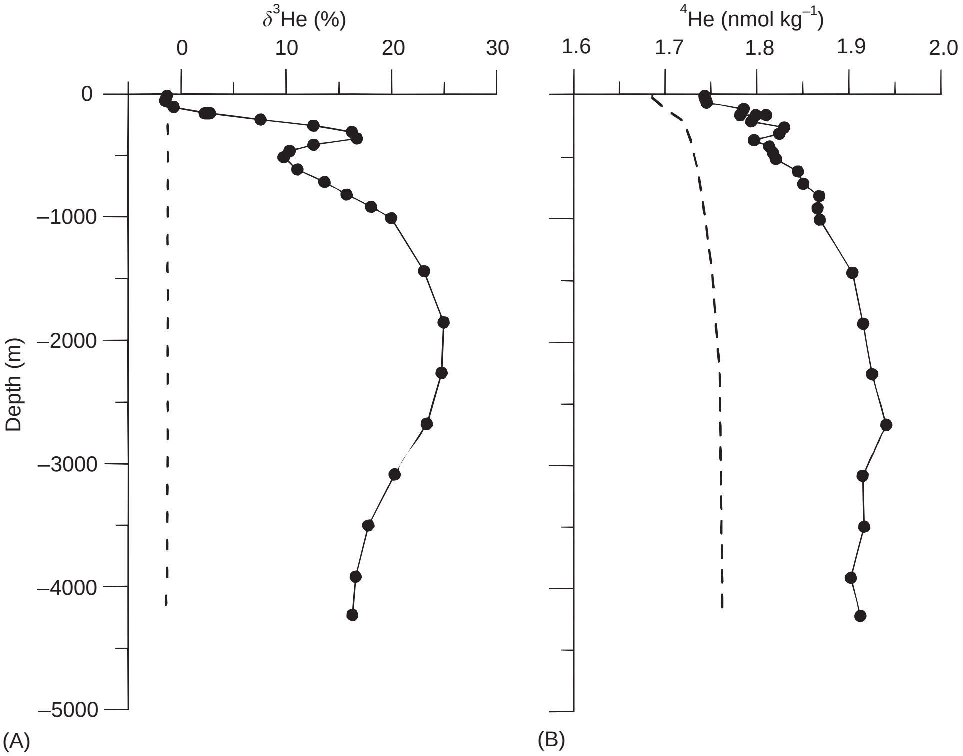

Figure 2 A typical helium profile collected at 28.5°N, 121.6°W in the north Pacific Ocean. (A) The ^{3}He/^{4}He ratio expressed as $\delta(^3\text{He})$% plotted versus depth. The sharp peak at ~ 350 m depth is due to tritium decay, while the broad maximum centered at ~ 2000 m depth is due to volcanic helium introduced along the mid-ocean ridge system. The dashed line represents the $\delta(^3\text{He})$ for sea water in equilibrium with air. (B) The ^{4}He concentration plotted versus depth for the same samples. The dashed line represents the ^{4}He concentration expected for sea water in equilibrium with air.

thin solid line corresponds to the atmospheric ratio ($^3\text{He}/^4\text{He} = 1.39 \times 10^{-6}$ or $R/R_A = 1$), and addition of air would cause the values to migrate along this line. As expected, the range of equilibrium solubility values falls directly on the atmospheric line. Although the measured samples (filled circles) near the ocean surface also fall on this line, the deeper samples fall off the atmospheric trend, defining a much steeper slope. This steeper slope is direct evidence that the helium that has been added to the deep ocean has a higher ^{3}He/^{4}He ratio than air.

Mid-ocean Ridge Helium

The input of volcanic helium has affected the helium content of all the major ocean basins, although the magnitude of this effect varies greatly. To a large degree, the amount of the excess volcanic helium in each of the ocean basins is controlled by the relative strength of the hydrothermal input, which is in turn roughly proportional to the spreading rate of the ridges. In the Pacific Ocean, where the fastest ridge-crest spreading rates are found, the ^{3}He/^{4}He values at mid-depth average $\delta(^3\text{He}) = 20\%$ for the entire Pacific basin (**Figure 4**). The Indian Ocean, which has ridges spreading at intermediate rates, has $\delta(^3\text{He})$ values averaging about 10–15%. Finally, the Atlantic Ocean, which is bisected by the slow-spreading Mid-Atlantic Ridge, has the lowest ^{3}He enrichments, averaging $\delta(^3\text{He}) = 0$–5% (**Figure 4**).

It has been recognized for several decades that the distribution of mantle ^{3}He has great potential for delineating the patterns of circulation and mixing of deep and intermediate water masses. This potential is probably greatest in the Pacific Ocean, because of the strong ^{3}He signal in that ocean. The helium field at mid-depth in the Pacific has been mapped in considerable detail (**Figure 5**). This work has identified several distinct helium plumes emanating from active hydrothermal systems distributed along the mid-ocean ridges. In the eastern equatorial Pacific, two jets of helium-rich water originate at latitude 10°N and at 14°S on the crest of the East Pacific Rise (EPR) and protrude westward into the interior of the basin. Between these two helium jets there is a minimum in the ^{3}He signal on the Equator. This distinct pattern in the helium distribution requires westward transport at mid-depth in the core of

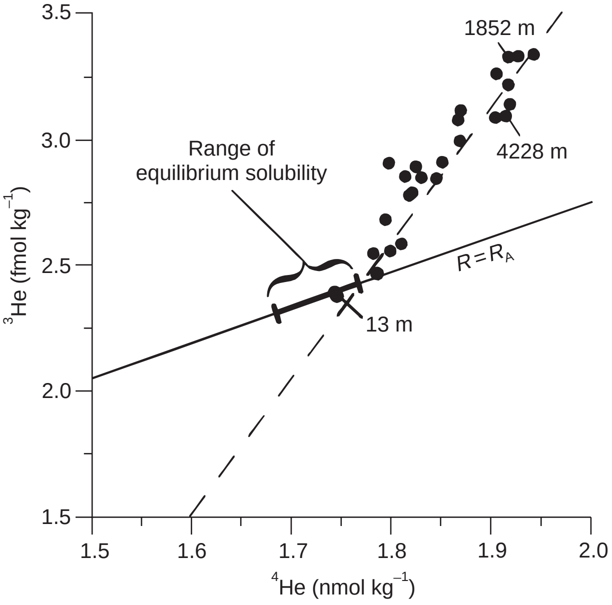

Figure 3 The ^{3}He concentration (in fmol kg^{-1} or 10^{-15} mol kg^{-1}) plotted versus ^{4}He concentration (in nmol kg^{-1} or 10^{-9} mol kg^{-1}) for the samples shown in **Figure 2**. In this plot the slope of any trend corresponds to the isotopic ratio of the end-member helium that has been added to the water samples. The depths in meters of three representative samples are indicated. The thick solid line represents the range of equilibrium solubility values expected for air saturated water (Weiss, 1970; 1971). As expected, the equilibrium solubility values fall on the thin solid line, which is the mixing relation expected for air helium ($R = R_A$). The steep slope of the dashed line, which is a best fit to the sea water samples, indicates that helium with an elevated ^{3}He/^{4}He ratio ($R > R_A$) has been added.

these helium plumes, and suggests eastward transport on the Equator (see dashed arrows in **Figure 5**). A separate helium plume is present in the far northeast Pacific produced by input on the Juan de Fuca and Gorda Ridges (JdFR). Although this helium signal is weaker than the helium plumes from the EPR, the JdFR helium is still traceable as a distinct plume that trends south-west into the interior of the north Pacific basin. Farther south at ~20°N, a low-^{3}He tongue penetrates from the west, implying eastward transport at this latitude. Thus the helium field defines a cyclonic (clockwise) circulation pattern at ~2000 m depth in the northeast Pacific.

Hot Spot Helium

In addition to the volcanism along the global mid-ocean ridge system, the oceans are also affected by hot spot volcanoes. Over 100 hot spots have been identified on the Earth's surface, and many of them are located within the ocean basins. One of the best-known examples is the Hawaiian hot spot, which over time has generated the Hawaiian Islands and the Hawaiian-Emperor seamount chain. Unlike mid-ocean ridges, which are submarine, many hot spot volcanoes are subaerial and do not necessarily have direct input into the oceans. Furthermore, hot spot volcanoes have not been explored extensively for their volcanic and hydrothermal activity. Nevertheless, there are several known examples of submarine hydrothermal input at hot spots. Macdonald Seamount in the south Pacific has active vents on its summit that inject volatiles into the overlying water column at a depth of ~130 m. Loihi Seamount, situated on the south-eastern flank of the island of Hawaii, also has active vents near its summit at a depth of ~1000 m. Loihi is of considerable importance because it is thought to be the current

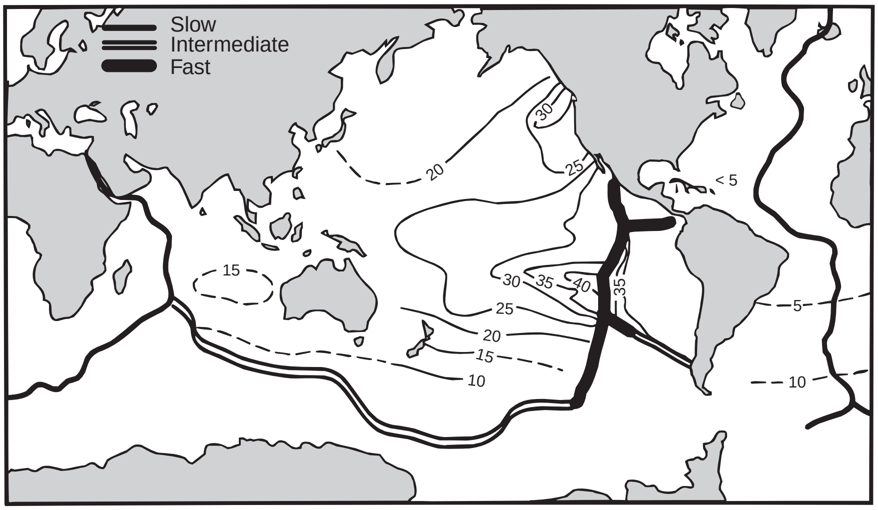

Figure 4 Map of $\delta(^3\text{He})\%$ at mid-depth in the world ocean. The location of the mid-ocean ridges is shown, and the relative spreading rate is indicated by the width of the lines.

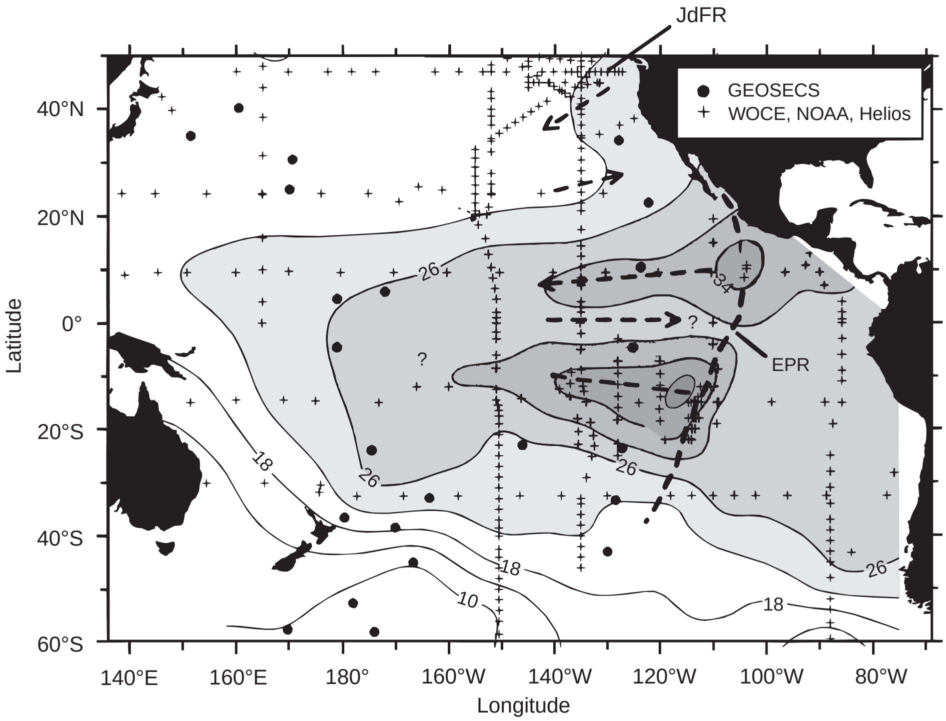

Figure 5 Map of $\delta(^3\mathrm{He})\%$ contoured on a surface at 2500 m depth in the Pacific. Contour interval is 4%. The major helium sources lie along the East Pacific Rise (EPR) and the Juan de Fuca Ridge (JdFR) systems. The dashed arrows indicate areas where the helium plumes define regional circulation patterns. Data along WOCE lines P4 and P6 are from Jenkins (unpublished data). All other data are from Lupton (1998).

locus of the Hawaiian hot spot. Loihi lavas and hydrothermal fluids contain helium with a very primitive signature of $R/R_A = 25\text{–}30$, indicating a deep mantle origin.

It has been known for some time that hydrothermal venting on Loihi Seamount produces water column plumes that can be detected with tracers such as temperature, manganese, iron, and methane.

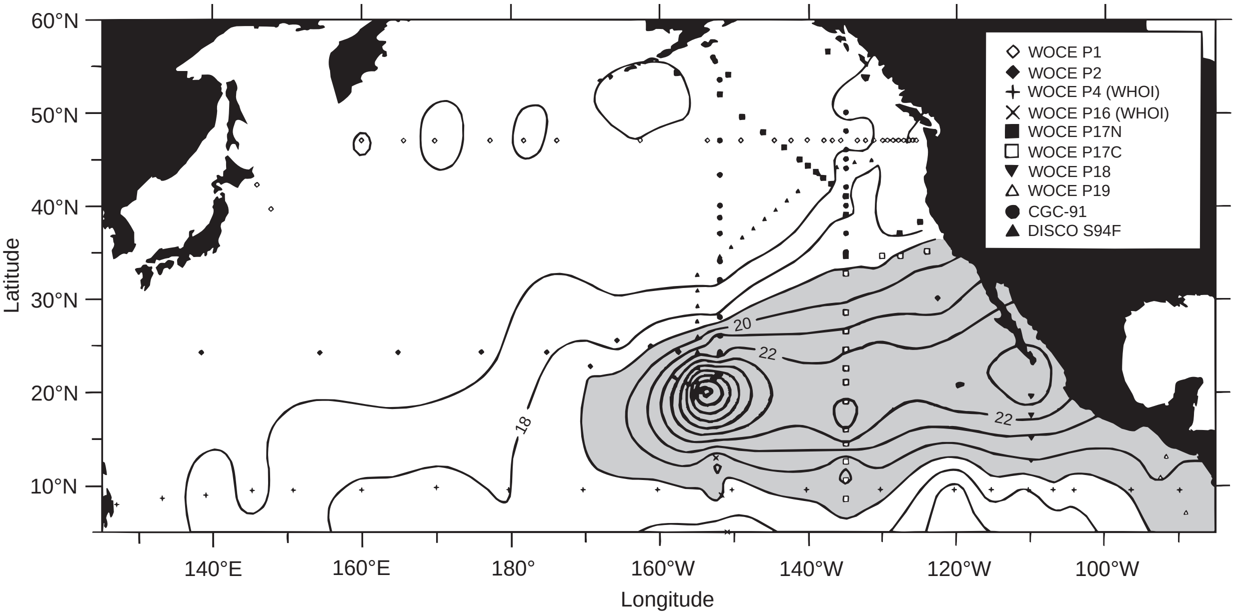

Figure 6 Map of $\delta(^3\mathrm{He})\%$ contoured on a surface at 1100 m depth in the north Pacific, showing the broad lateral extent of a helium plume emanating from Loihi Seamount on the south-eastern flank of the Island of Hawaii. As indicated in the key, data are from several different expeditions.

However, these tracers are not useful for far-field studies of the Loihi plume because they are either rapidly removed from the water column or are present in low concentrations. Because helium is a stable, conservative tracer that is highly enriched in Loihi vent fluids, the helium signal from Loihi is detectable at considerable distances from the Hawaiian Islands. As shown in **Figure 6**, a map of $\delta(^3\mathrm{He})$ on a surface at 1100 m depth reveals a ^{3}He-rich plume that extends eastward from the Hawaiian Islands for several thousand kilometers, reaching the coast of Mexico at its greatest extent. This far-field plume produced by the Hawaiian hot spot clearly defines an eastward transport at ~1000 m depth in this region of the north Pacific. Furthermore, because the end-member helium introduced at Loihi has a ^{3}He/^{4}He ratio three times higher than mid-ocean ridge helium, it should be

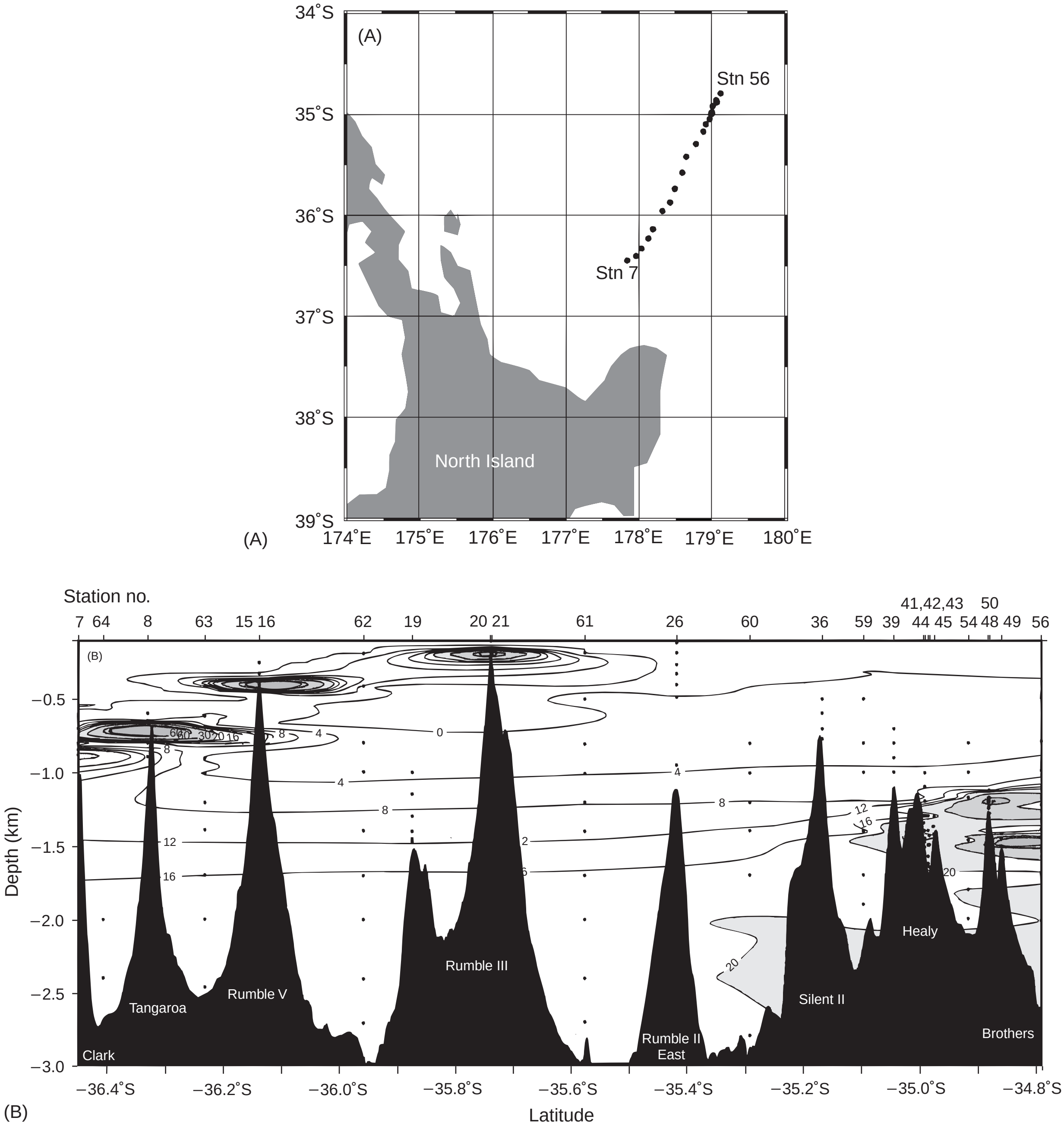

Figure 7 (A) Map showing location of hydrographic stations along the southern end of the Kermadec Arc northeast of New Zealand. (B) $\delta(^3\mathrm{He})\%$ contoured in section view along the southern end of the Kermadec Arc, showing ^{3}He-rich water-column plumes emanating from several of these subduction zone volcanoes. From de Ronde *et al.* (2000).

possible to distinguish the Loihi helium from mid-ocean ridge helium with accurate measurements of ^{3}He and ^{4}He concentrations. The ability to distinguish hot spot helium from mid-ocean ridge helium has been demonstrated for the Loihi helium plume near Hawaii but not yet in the far-field.

Subduction Zone Helium

Submarine volcanism also occurs along convergent margins, particularly in regions where two oceanic plates are converging. However, very little is known about the incidence of submarine hydrothermal activity associated with this type of volcanism. Studies of subaerial volcanoes at convergent margins have shown that these volcanoes emit mantle helium with an isotopic ratio of $R/R_A = 3$–7, lower than in mid-ocean ridges. Thus the volcanic helium from subduction zones represents a third type of mantle helium that is isotopically distinct from mid-ocean ridge and hot spot helium.

One clear example of oceanic helium plumes from subduction zone volcanism is shown in **Figure 7**, which shows the results of a survey along the southern end of the Kermadec Arc northeast of New Zealand. The Kermadec Arc consists of a series of discrete volcanoes generated by the subduction of the Pacific plate beneath the Australian plate. At the southern end of the arc these volcanoes are submarine, while farther north some of them are subaerial volcanoes, including Curtis Island, Macauley Island, and Raoul Island. The survey shown in **Figure 7** consisted of a series of hydrographic casts along the arc, and many of the casts were lowered directly over the summits of these arc volcanoes. The section shown in **Figure 7B** shows a series of ^{3}He-rich plumes emanating from several of these volcanoes. Furthermore, the plumes are found at a variety of depths between 150 m for Rumble III volcano down to 1400 m for Brothers volcano. A plot of ^{3}He versus ^{4}He concentration for these samples (not shown), indicated an average ^{3}He/^{4}He ratio of $R/R_A = 6$, in agreement with previous studies of helium from subaerial subduction zone volcanoes. Although the lateral extent of the helium plumes from the Kermadec Arc is not known, this survey confirms that subduction zone volcanoes do produce helium plumes that can be used to trace ocean currents. Furthermore, these subduction zone plumes are potentially quite valuable for tracer studies, since they occur at a wide variety of depths and are generally much shallower than plumes produced at mid-ocean ridges (**Figure 7B**).

See also

Current Systems in the Atlantic Ocean. Current Systems in the Indian Ocean. Hydrothermal Vent Deposits. Hydrothermal Vent Fluids, Chemistry of. Mid-ocean Ridge Geochemistry and Petrology. Mid-ocean Ridge Tectonics, Volcanism and Geomorphology. Noble Gases and the Cryosphere. Ocean Circulation. Propagating Rifts and Microplates. Seamounts and Off-ridge Volcanism. Thermohaline Circulation. Tritium–Helium Dating.

Further Reading

Clarke WB, Beg MA and Craig H (1969) Excess ^{3}He in the sea: evidence for terrestrial primordial helium. *Earth and Planetary Science Letters* 6: 213–220.

Craig H, Clarke WB and Beg MA (1975) Excess ^{3}He in deep water on the East Pacific Rise. *Earth and Planetary Science Letters* 26: 125–132.

Craig H and Lupton JE (1981) Helium-3 and mantle volatiles in the ocean and the oceanic crust. In: Emiliani C (ed.) *The Sea*, vol. 7, pp. 391–428. New York: Wiley.

Krylov A Ya, Mamyrin BA, Khabarin L, Maxina TI and Silin Yu I (1974) Helium isotopes in ocean floor bedrock. *Geokhimiya* 8: 1220–1225.

Lupton JE (1983) Terrestrial inert gases: isotope tracer studies and clues to primordial components in the mantle. *Annual Review of Earth and Planetary Science* 11: 371–414.

Lupton JE (1995) Hydrothermal plumes: near and far field. In: Humphris S *et al.* (eds) *Seafloor Hydrothermal Systems, Physical, Chemical, Biological, and Geological Interactions*, Geophysical Monograph Series, vol. 91, pp. 317–346. Washington, DC: American Geophysical Union.

Lupton JE (1998) Hydrothermal helium plumes in the Pacific Ocean. *Journal of Geophysical Research* 103: 15855–15868.

Lupton JE and Craig H (1975) Excess ^{3}He in oceanic basalts: evidence for terrestrial primordial helium. *Earth and Planetary Science Letters* 26: 133–139.

Suess HE and Wänke H (1965) On the possibility of a helium flux through the ocean floor. *Progress in Oceanography* 3: 347–353.

Weiss RF (1970) Helium isotope effect in solution in water and seawater. *Science* 168: 247–248.

Weiss RF (1971) Solubility of helium and neon in water and seawater. *Journal of Chemical Engineering Data* 16: 235–241.